# On-Line, Kinodynamic Trajectory Generation Through Rectangular Channels Using Path and Motion Primitives

Efstathios Bakolas and Panagiotis Tsiotras

***Abstract*— We present a motion planning scheme for ground vehicles operating in a partially known environment. Kinematic constraints stemming from vehicle dynamics and from the requirement that the path must remain inside a free channel of a rectangular cell decomposition of the environment at all times, are dealt with by constructing a time-parameterized path using an appropriate combination of a finite number of path and motion primitives. This simplifies considerably the motion planning problem and, furthermore, reduces the computational cost of replanning at each time instant. Our analysis also provides closed-form expressions on the size of each cell so that the ensuing cell decomposition is compatible to the vehicle dynamics.**

## I. Introduction

The importance of taking into account limitations over the steering capacity of typical ground vehicles, and especially car-like robots, is well known in the area of motion planning. One common approach typically employed to account for this problem is the design of geometric paths with bounded curvature. For the case of an obstacle-free environment, curvature-constrained paths of minimal length, and with prescribed initial and final positions and tangents, have been characterized in [1] and [2] for the 2D (planar) and the 3D case, respectively. In the presence of obstacles, the problem of the shortest, curvature-constrained path becomes extremely complicated. Actually, the planar, shortest, curvature-constrained path problem is, in general, NP hard [3]. The case of polygonal obstacles was investigated for the first time by Jacobs and Canny [4], who proved that the existence of a curvature-constrained planar path, with prescribed initial and final positions and orientations, implies the existence of a shortest-length curvature-constrained planar path, which satisfies the same boundary conditions. The recent work in [5], [6] deals with the geometric construction of curvature-constrained curves of "short" length inside narrow corridors.

The aforementioned methods tend to construct paths or trajectories that may be incompatible with the actual vehicle dynamics. Feasible paths need to take into account the vehicle dynamics. Algorithms based on optimal control theory can be used to solve the motion planning problem in the presence of input and path constraints, and are well known to the motion planning community. Examples include references [7], [8], [9], [10]. Unfortunately, these exact methods are computationally prohibitive for real-time implementation. Another, also suboptimal, approach is the one developed in [11], where the authors propose a hierarchical control architecture for maneuvering helicopters operating at the edge of their flight envelope, by discretizing the trajectory space into a finite number of steady-state (trim) conditions and (finite-time) maneuvers, the latter used to connect the trim trajectories.

Our work in this paper borrows from the same ideas as in [11], [12] in order to develop a kinodynamic planning scheme that is compatible with cell-based discrete path planning algorithms. This is achieved into two steps. At the first step, we construct a path $\mathsf{P}(s)$ that lies inside the narrow corridor defined by the channel of cells to the goal destination, and which adheres to the kinematic and curvature constraints imposed on the vehicle either by the mission objective, engine characteristics, or the environment (i.e., surface friction). The path $\mathsf{P}(s)$ is composed of a suitable combination of circular arcs and line segments, which are the *path primitives* of our scheme. In the second step, we impose a time parametrization along this path by selecting the control inputs required for the vehicle to reach the goal destination along the path $\mathsf{P}(s)$ in minimum-time. Again, we do this for each path primitive (subject to the correct and consistent boundary conditions) thus resulting in a family of *motion primitives*, whose suitable combination via a receding horizon scheme yields a nearly-optimal trajectory. The approach is numerically efficient and suitable for on-line implementation with limited computational resources. Furthermore, the short horizon required implementing the proposed strategy makes the whole planning scheme flexible and responsive to environmental changes.

## II. Kinematic Model

Let us consider the motion of a ground vehicle of unit mass moving along a planar curve $\alpha : \mathcal{I} \mapsto \mathbb{R}^2$, which is acted upon by the force components $f_t = \dot{v}$ in the tangential direction and $f_r = v\omega$ in the normal (radial) direction. The motion of the vehicle is given by the equations

$$\ddot{x}(t) = \dot{v}(t)\cos\theta(t) - v(t)\omega(t)\sin\theta(t), \tag{1}$$

$$\ddot{y}(t) = \dot{v}(t)\sin\theta(t) + v(t)\omega(t)\cos\theta(t), \tag{2}$$

$$\dot{\theta}(t) = \omega(t). \tag{3}$$

In equations (1)-(3) $x, y$ are the cartesian coordinates of the vehicle, $\theta$ is the heading angle of the velocity vector (always tangent to $\alpha$), $v$ is the vehicle's speed and $\dot{v}, \omega$ are the control inputs. The set of admissible inputs $\mathbf{U}$ for the

E. Bakolas is a Ph.D. candidate at the School of Aerospace Engineering, Georgia Institute of Technology, Atlanta, GA 30332-0150, USA, Email: gth714d@mail.gatech.edu

P. Tsiotras is a Professor at the School of Aerospace Engineering, Georgia Institute of Technology, Atlanta, GA 30332-0150, USA, Email: tsiotras@gatech.edu

vehicle is given by

$$\mathbf{U} \triangleq \left\{ (\dot{v}, \omega) : \left( \frac{\dot{v}}{f_t^{\max}} \right)^2 + \left( \frac{v\omega}{f_r^{\max}} \right)^2 \leq 1 \right\}. \quad (4)$$

We also assume that the speed of the vehicle is bounded both from above and below as follows

$$v(t) \in [v_{\min}, v_{\max}], \qquad t \geq 0. \quad (5)$$

Our objective is to derive constraints over the geometric characteristics of the curves the vehicle is capable of tracking, so that later on we can propose a path generation scheme that is compatible with the kinodynamic and input constraints induced by the relations (4) and (5). In particular, since $|\omega(t)| = \kappa(s(t))v(t)$, where $\kappa(s) \geq 0$ and $s$ are the curvature and the arc length of the ensuing path respectively, inequality (4) implies that $v^2(t)\kappa(s) \leq f_r^{\max}, \quad t \geq 0$.

We can thus derive an upper bound over the speed of the vehicle along the path as a function of the force envelope and the curvature $\kappa(s)$ of the path. We call this speed the *critical* speed $v_{\mathsf{c}}$, defined by

$$v_{\mathsf{c}}(s) = \begin{cases} \sqrt{\dfrac{f_r^{\max}}{\kappa(s)}}, & \sqrt{\dfrac{f_r^{\max}}{\kappa(s)}} \in [v_{\min}, v_{\max}], \\ v_{\max}, & \sqrt{\dfrac{f_r^{\max}}{\kappa(s)}} > v_{\max}. \end{cases} \quad (6)$$

Alternatively, the set of path curves that can be tracked exactly by the vehicle is restricted by the point-wise maximum allowable curvature $\kappa_{\max}$ , where $\kappa_{\max} \leq f_r^{\max}/v_{\min}^2$.

## III. Path Planning Using Path Primitives

Any local path planning scheme that is based on combinations of a finite number of path primitives, has to deal with situations where the boundary and/or interior conditions of the problem at different time instants may be incompatible with one another. Thus, what we need is an efficient way to generate, and smoothly join together, (time-parameterized) path segments.

In the sequel, we assume that the agent has detailed knowledge of the environment over an horizon of only three cells. Let $\mathcal{A}$ denote the cell occupied by the vehicle at a given time instant $t$. Any feasible channel $\mathcal{M}$ comprised of three consecutive free cells, namely $\mathcal{A}$, $\mathcal{B}$ and $\mathcal{C}$, forms the horizon of the continuous motion planning problem at the given time instant $t$. We assume that this horizon is identical to the exploration horizon of the vehicle on-board sensors; hence the cells $\mathcal{A}$, $\mathcal{B}$ and $\mathcal{C}$ are the only free cells at the time instant $t$. All cells outside the horizon of the on-board sensors are assumed to be mixed. We further assume that, at each time $t$, a channel of cells $\mathcal{M}_{g,t}$ (comprised of free and mixed cells) to the goal destination is known, such that $\mathcal{M} \subset \mathcal{M}_{g,t}$. The channel $\mathcal{M}_{g,t}$ may be constructed by any local discrete planning algorithm (e.g., [13], [14]) that solves the geometric path planning problem at the cell level each time the algorithm is executed.

### A. Constructing the Path $\mathsf{P}(s)$ Inside the Free Cells of $C_d$

Let $C_d$ denote a uniform square cell decomposition of cell size $\ell$ with a 4-connectivity scheme. We introduce the *parent local channels* $\mathcal{M}_1^p$, $\mathcal{M}_2^p \subset \mathbb{R}^2$ that are shown in Fig. 1. Any arbitrary 3-cell local channel $\mathcal{M}$ can be deduced by either the parent local channel $\mathcal{M}_1^p$ or $\mathcal{M}_2^p$ by means of plane isometries.

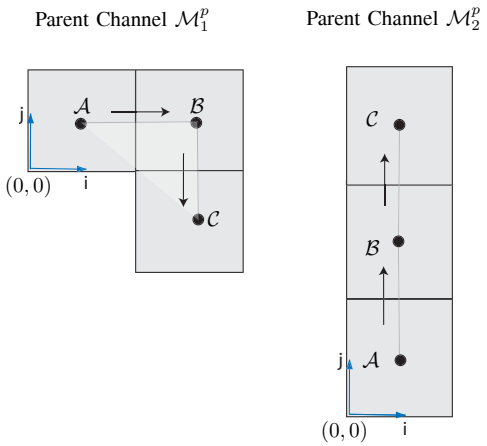


Fig. 1. Parent channels of three cells.

In order to generate the route of the vehicle inside the narrow corridor, which is represented by a channel of cells, we concatenate locally shortest-length, curvature-constrained paths, which, in turn, are composed of line segments and circular arcs. Let us consider the case when the agent enters a free cell $\mathcal{A}$ of $\mathcal{M}$ at some point along the West edge and exits $\mathcal{A}$ from a point along either the East or South edge. To the entrance and exit edges of $\mathcal{A}$ we associate two circles, $\mathcal{C}_1$ and $\mathcal{C}_{2,a}$ or $\mathcal{C}_1$ and $\mathcal{C}_{2,b}$, located at the midpoints of the West and the East or South edge, respectively. The circles $\mathcal{C}_1$ and $\mathcal{C}_{2,a}$ or $\mathcal{C}_1$ and $\mathcal{C}_{2,b}$ can be joined by either one of the four common tangent line segments $\mathcal{Y}_{12}$ or a circle $\mathcal{C}_{12}$ or a composite path that is composed of a circle $\mathcal{C}_{12,a}$ a line segment $\mathcal{Y}_{12}$ and a second circle $\mathcal{C}_{12,b}$. See Fig. 2.

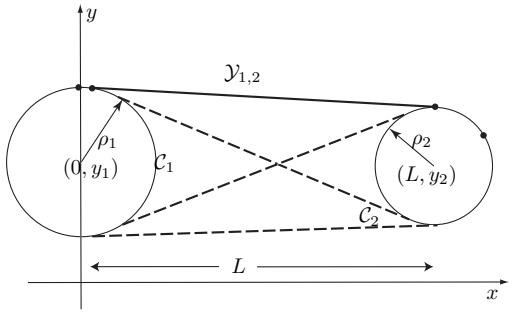


Fig. 2. Geometric path generation problem. The problem is well defined as long as $\rho_1 + \rho_2 \leq L$.

The assumption here is that the agent enters each cell either by performing a steady turn or moving along a rectilinear path. The resulting path is a composite curve $\alpha$, we write $\alpha = \mathcal{C}_1 \circ \mathcal{K}_{12} \circ \mathcal{C}_2$ where $\mathcal{K}_{12} \in \{\mathcal{Y}_{12}, \mathcal{C}_{12}, \mathcal{C}_{12,a} \circ \mathcal{Y}_{12} \circ \mathcal{C}_{12,b}\}$ where $\circ$ denotes curve composition.

For the rest of this paper we shall concentrate our analysis for the case $\mathcal{K}_{12} = \mathcal{Y}_{12}$ for simplicity. Figure 3 shows all feasible paths inside the two parent local channels composed of locally length-optimal paths. For the shake of clarity, all the maneuvers depicted in Figure 3 involve circles whose centers are located at the middle points of the corresponding edges.

### B. Path Generation Algorithm

Without loss of generality, assume that $\mathcal{M} \cong \mathcal{M}_1^p$ as in Fig. 4. Since the path inside the cell $\mathcal{A}$ is uniquely determined by the entry velocity, the first part of the composite path is constructed immediately. Note that neither the exit velocity nor the exit edge from cell $\mathcal{C}$ is known at that point, since not all of the neighbors of the cell $\mathcal{C}$ are expanded at that point. When the vehicle enters the cell $\mathcal{B}$, all the neighbors of the cell $\mathcal{C}$ are expanded. Furthermore, a new channel of three adjacent cells becomes available from the higher level discrete local path planning algorithm. This new channel $\widetilde{\mathcal{M}}$ is comprised of the cells $\mathcal{B}$ and $\mathcal{C}$ of the channel $\mathcal{M}$ plus the new cell $\mathcal{A}'$, which is adjacent to the $\mathcal{C}$ cell. The exit edge from cell $\mathcal{C}$ is now available. Thus, the exit velocity is $O_{i,j}$, where the index $i$ is fixed but the $j$ index is still unknown. The knowledge of the exit edge form cell $\mathcal{C}$ suffices to determine the path inside $\mathcal{B}$ uniquely. Finally, when the agent enters the cell $\mathcal{C}$ the exit velocity from the channel $\widetilde{\mathcal{M}}$ finally becomes available. The situation can be better understood with the simple example depicted in Fig. 4. At the time the vehicle enters the cell $\mathcal{C}$, the two cells $\mathcal{A}'$ and $\mathcal{B}'$ within the exploration horizon of the vehicle become available. The local channel $\widetilde{\mathcal{M}}$ is composed of the cells $\mathcal{C}$, $\mathcal{A}'$ and $\mathcal{B}'$ with $\widetilde{\mathcal{M}} \cong \mathcal{M}_1^p$. The path inside $\mathcal{A}'$ is then specified in accordance with Fig. 3. Hence, the path inside $\mathcal{A}'$ is restricted to be one of the dashed curves given in Fig. 4. Therefore, there exists only one output orientation from the local channel $\widetilde{\mathcal{M}}$ that is compatible with the allowable path switches. Consequently, the path-planning inside $\mathcal{M}$ is completed. The exit velocity from cell $\mathcal{C}$ will be the input orientation for the new local channel $\mathcal{M}'$, composed of the cells $\mathcal{A}'$, $\mathcal{B}'$ and the new cell $\mathcal{C}'$, which is adjacent to $\mathcal{B}'$. This results in a new problem similar to the class of problems depicted in Fig. 3. The same procedure is applied repeatedly until the vehicle reaches the goal destination. Using this scheme we can generate the composite path $\mathsf{P}(s)$, which is a finite composition of curves $\alpha_j = \mathcal{C}_j \circ \mathcal{Y}_{j,j+1} \circ \mathcal{C}_{j+1}$, for $j = 1, \ldots, n$ where $n$. Subsequently, we may write the overall generated path as $\mathsf{P}(s) = \alpha_1(s) \circ \cdots \circ \alpha_n(s)$.

### C. Complexity Estimates

We assume that the free space in the vicinity of the vehicle is represented via a cell decomposition which induces a grid of mesh $\ell^2$, where $\ell$ is the size of each cell, whereas the rest of the world is represented via a grid of mesh $\Lambda^2$, where, typically, with $\ell \ll \Lambda$. Let us assume that the obstacle space of our problem is composed of polygonal obstacles and let $N$ be the total number of corners of all these obstacles. The number of free cells cannot be more than $\mathcal{O}(\eta^2 N^2/\ell^2)$ whereas the number of mixed cells cannot exceed $\mathcal{O}(N^2/\Lambda^2)$, where $\eta \sim \mathcal{O}(\ell^2/\Lambda^2)$ is the ratio of the exploration horizon over the total area of the world. We store the free cells in a balanced binary tree and we lookup the four neighbors of each cell. We put pointers to the neighbors that have been expanded. The running time of this step is $\mathcal{O}\left(\ell^2 N^2/\Lambda^4\right)$. The channel of free and mixed cells to the goal destination is constructed every time by performing a search using $A^*$ or Dijkstra's algorithm. This search typically requires a running time of order $\mathcal{O}(\ell^2 N^2/\Lambda^4 \log(\ell^2 N^2/\Lambda^4))$. The selection of the maneuver to execute each time a new cell becomes available is unique and of constant time, that is, of order $\mathcal{O}(1)$. If we now assume that the total number of the cells that the vehicle visits during its route to the goal destination is $n$, the previous steps are executed $\mathcal{O}(n)$ number of times. On the other hand, it can be easily shown that a brute force method, which at each step checks every route comprised of curves made up from the available path primitives in the library, would require running time $\mathcal{O}(n)$ instead of $\mathcal{O}(1)$. Hence, a brute force method would normally require an additional running time overhead of order $\mathcal{O}(n^2)$ instead of $\mathcal{O}(n)$.

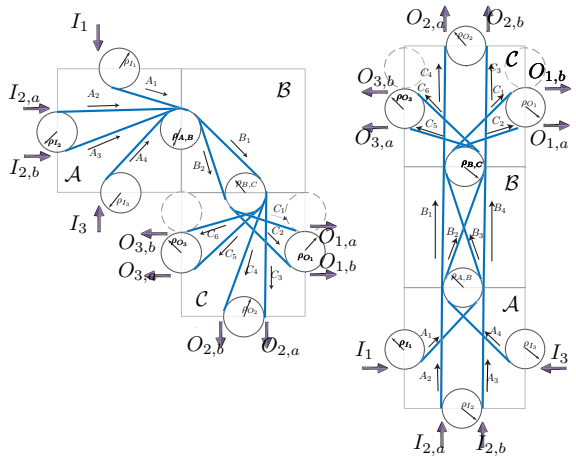


Fig. 3. Feasible maneuvers inside the parent cell channels $\mathcal{M}_1^p$ and $\mathcal{M}_2^p$.

## IV. From Paths to Trajectories: Time Optimal Control

In this section we solve the time optimal control problem for the system (1)-(3) along the composite path $\mathsf{P}(s) = \alpha_1(s) \circ \cdots \circ \alpha_n(s)$ under the constraints (4) and (5). Along the given path $\mathsf{P}(s)$, both the equations of motion and the constraints are significantly simplified. In particular, while the agent moves along one of the straight line segments $\mathcal{Y}_{j,j+1}$ of $\mathsf{P}(s)$, the equations of motion are given by

$$\ddot{s}(t) = u(t) \qquad \dot{\theta}(t) \equiv 0, \tag{7}$$

where $u(t) = \dot{v}(t)$ is the control input, along with the constraints (5) and

$$|u(t)| \leq f_t^{\max}. \tag{8}$$

Additionally, when the agent traverses a circular arc of $\mathcal{C}_j$ with radius $\rho_j$, the simplified equations of motion are given

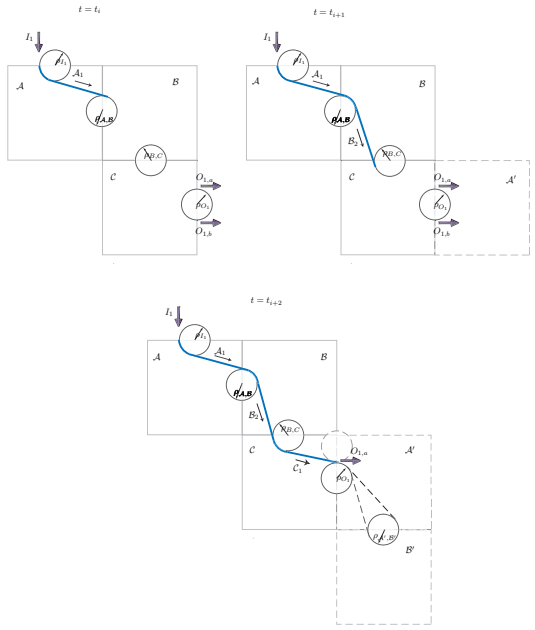

Fig. 4. The construction of the trajectory inside the channel $\mathcal{M}$.

by

$$\dot{\theta}(t) = \omega(t), \tag{9}$$

along with the constraint

$$\left(\frac{\dot{\omega}(t)\rho_j}{f_t^{\max}}\right)^2 + \left(\frac{\omega^2(t)\rho_j}{f_r^{\max}}\right)^2 \leq 1. \tag{10}$$

Furthermore, the critical speed is constant, and is defined by

$$v_{\mathsf{c}}^{\mathcal{C}_j} = \sqrt{f_r^{\max}\rho_j}, \qquad j = 1, 2, \ldots, n+1. \tag{11}$$

The constraints in (8) and (10) specify the set of admissible control inputs $\mathcal{U}_j \subset \mathbf{U}$, $j = 1, 2$, associated to the motion of the vehicle along any line segment and circular arc of the path $\mathsf{P}(s)$ respectively with $\mathcal{U}_1 \bigcap \mathcal{U}_2 = \emptyset$. Let $\mathcal{U} = \mathcal{U}_1 \bigcup \mathcal{U}_2 = \mathbf{U} \subset \mathbb{R}^2$ be the set of admissible inputs associated to the motion of the vehicle along the path $\mathsf{P}(s)$.

We consider the following optimal control problem for the motion of a particle that tracks *exactly* the composite path $\mathsf{P}(s)$ at minimum time.

*Problem 1:* Given the system described by equations (7) along any line segment $\mathcal{Y}_{j,j+1} \in \mathsf{P}(s)$ and by equation (9) along any circular arc $\mathcal{C}_j \in \mathsf{P}(s)$, and the cost functional

$$J(\mathsf{u}) = \int_0^{S_f} \frac{\mathrm{d}s}{v(s)} = T_f, \tag{12}$$

determine the control input $\mathsf{u}^*_{[0,T_f]} = \left(u^*_{[0,T_f]}, \omega^*_{[0,T_f]}\right)^{\mathsf{T}}$, such that

1) The control $\mathsf{u}^*_{[0,T_f]}$ belongs to the set of admissible inputs $\mathcal{U}_2$.
2) The trajectory $(s^*(t), v^*(t), \theta^*(t))^{\mathsf{T}}$ generated by the control $\mathsf{u}^*_{[0,T_f]}$ satisfies
   a) The boundary conditions $s^*(0) = 0$, $v^*(0) = v_{\mathsf{c}}^{\mathcal{C}_1} = \sqrt{f_r^{\max}\rho_1}$, $\theta^*(0) = \left\{-\frac{\pi}{2}, 0, \frac{\pi}{2}, \pi\right\}$, $s^*(T_f) = S_f$.
   b) The global point-wise inequality constraint (5).
3) The control $\mathsf{u}^*_{[0,T_f]}$ minimizes the cost functional $J(\mathsf{u})$ given in (12).

The following assumption allows us to work with extremely short execution horizons (just three cells) for the minimum-time Problem 1.

**Assumption 1.** *The vehicle reaches each circular arc $\mathcal{C}_j \in \mathsf{P}(s)$ of radius $\rho_j$ with the corresponding critical speed $v_{\mathsf{c}}^{\mathcal{C}_j} = \sqrt{f_r^{\max}\rho_j}$.*

Under Assumption 1, the minimum-time problem along the circular arcs of the path $\mathsf{P}(s)$ can be solved explicitly. In particular, the vehicle tracks the circular arc of radius $\rho_j$ with constant speed, which is equal to the critical speed $v_{\mathsf{c}}^{\mathcal{C}_j}$. Hence the speed of the vehicle is point-wise maximized along the circular arcs of the composite path $\mathsf{P}(s)$. By Bellman's principle of optimality, the trajectory generated by applying $\dot{v} = 0$ and $\omega = \sqrt{f_r^{\max}/\rho_j}$ along the circular arc $\mathcal{C}_j$, where $j = 1, \ldots, n+1$, is optimal. Therefore, we only need to solve the minimum-time problem on each line segment $\mathcal{Y}_{j,j+1}$ connecting two successive circles $\mathcal{C}_j$ and $\mathcal{C}_{j+1}$ of radii $\rho_j$ and $\rho_{j+1}$, with the appropriate boundary conditions. To this end, we formulate the following minimum-time problem along the line segment $\mathcal{Y}_{j,j+1}$ that connects the circles $\mathcal{C}_j$ and $\mathcal{C}_{j+1}$.

*Problem 2:* Let $\bar{s}_{j,1}$ and $\bar{s}_{j+1,2}$ be the $s$-coordinates of the point of departure from $\mathcal{C}_j$ and the point of arrival at $\mathcal{C}_{j+1,2}$ and $\bar{t}_{j,1,1}$ and $\bar{t}_{j,2}$ be the corresponding time instants. Determine the control input $\mathsf{u}^*_{[\bar{t}_{j,1},\bar{t}_{j+1,2}]}$ that solves the minimum-time Problem 1 along $\mathsf{P}(s)$ for $s \in [\bar{s}_{j,1}, \bar{s}_{j+1,2}]$ with the boundary conditions $v^*(\bar{t}_{j,1}) = v_{\mathsf{c}}^{\mathcal{C}_j}$ and $v^*(\bar{t}_{j+1,2}) = v_{\mathsf{c}}^{\mathcal{C}_{j+1}}$.

In order to derive candidate solutions for this minimum-time problem, we use an argument based on the point-wise maximization of the speed along the path [7], [10]. In particular, a vehicle travelling initially with speed $v_{\mathsf{c}}^{\mathcal{C}_j}$ begins to accelerate at $s = \bar{s}_{j,1}$ with maximum acceleration $f_t^{\max}$ until it reaches the maximum speed $v_{\max}$ at $s = s_{\gamma_j}$, at time $t = t_{\gamma_j}$, where $s_{\gamma_j}$ and $t_{\gamma_j}$ are given by

$$s_{\gamma_j} = \bar{s}_{j,1} + \frac{v_{\max}^2 - \left(v_{\mathsf{c}}^{\mathcal{C}_j}\right)^2}{2f_t^{\max}}, \qquad t_{\gamma_j} = \frac{v_{\max} - v_{\mathsf{c}}^{\mathcal{C}_j}}{f_t^{\max}}. \tag{13}$$

The vehicle then maintains maximum speed $v_{\max}$ until $s = s_{\delta_j}$, at time $t = t_{\delta_j}$, when it starts to decelerate with maximum deceleration $-f_t^{\max}$ so that it reaches the circle $\mathcal{C}_{j+1}$ with the corresponding critical speed $v_{\mathsf{c}}^{\mathcal{C}_{j+1}}$. It follows readily that

$$s_{\delta_j} = \bar{s}_{j+1,2} - \frac{v_{\max}^2 - \left(v_{\mathsf{c}}^{\mathcal{C}_j}\right)^2}{2f_t^{\max}}, \tag{14}$$

$$t_{\delta_j} = \frac{-2v_{\max}v_{\mathsf{c}}^{\mathcal{C}_j} + \left(v_{\mathsf{c}}^{\mathcal{C}_{j+1}}\right)^2 + \left(v_{\mathsf{c}}^{\mathcal{C}_j}\right)^2}{2f_t^{\max}v_{\max}} + \frac{(\bar{s}_{j+1,2} - \bar{s}_{j,1})}{v_{\max}}. \tag{15}$$

After some calculations, we find that the total time $T^*_{\mathcal{Y}_{j,j+1}}$ is given by

$$T^*_{\mathcal{Y}_{j,j+1}} = \frac{\left(v_{\max} - v_{\mathsf{c}}^{\mathcal{C}_j}\right)^2 + \left(v_{\max} - v_{\mathsf{c}}^{\mathcal{C}_{j+1}}\right)^2}{2 f_t^{\max} v_{\max}} + \frac{(\bar{s}_{j+1,2} - \bar{s}_{j,1})}{v_{\max}}. \quad (16)$$

The elapsed time $\mathsf{T}_{\mathcal{Y}_{j,j+1}}$ that corresponds to the motion of the vehicle along the line segment $\mathcal{Y}_{j,j+1}$ can also be given as a function of the speed $v$ and the path length $s$. In particular,

$$\mathsf{T}_{\mathcal{Y}_{j,j+1}}(s,v) = \begin{cases} \dfrac{v(s) - v_{\mathsf{c}}^{\mathcal{C}_j}}{f_t^{\max}}, & s \in [\bar{s}_{j,1}, s_{\gamma_j}), \\ t_{\gamma_j} + \dfrac{s - s_{\gamma_j}}{v_{\max}}, & s \in [s_{\gamma_j}, s_{\delta_j}), \\ t_{\delta_j} + \dfrac{v_{\max} - v(s)}{f_t^{\max}}, & s \in [s_{\delta_j}, \bar{s}_{j+1,2}], \end{cases}$$

The following proposition formalizes the previous discussion.

*Proposition 1:* The feedback control law

$$u^*(s) = \begin{cases} f_t^{\max}, & s \in [\bar{s}_1, s_{\gamma_j}) \\ 0, & s \in [s_{\gamma_1}, s_{\delta_j}) \\ -f_t^{\max}, & s \in [s_{\delta_j}, \bar{s}_2]. \end{cases} \quad (17)$$

is the minimum time control for Problem 2. Furthermore, the minimum time $T^*_{\mathcal{Y}_{j,j+1}}$ is given by (16).

*Proof:* The proof follows easily by observing that the continuously differentiable cost function defined by $\mathcal{J}^*(s,v^*) = T^*_{\mathcal{Y}_{j,j+1}} - \mathsf{T}_{\mathcal{Y}_{j,j+1}}(s,v^*)$, satisfies the Hamilton-Jacobi-Bellman equation along the trajectory generated by the control (17) and also satisfies the HJB boundary condition on $(\bar{s}_{j+1,2}, v_{\mathsf{c}}^{\mathcal{C}_{j+1}})$. ■

We can now present the main result of this section.

*Proposition 2:* The feedback control law

$$\mathsf{u}^*_{\mathcal{C}}(s) = \left(0, \operatorname{sign}(\theta'(s)) \sqrt{\frac{f_r^{\max}}{\rho_j}}\right)^{\mathsf{T}}, s \in [\bar{s}_{j,2}, \bar{s}_{j,1}], \quad (18)$$

$$\mathsf{u}^*_{\mathcal{Y}}(s) = (u^*(s), 0)^{\mathsf{T}}, \ s \in [\bar{s}_{j,1}, \bar{s}_{j+1,2}], \quad (19)$$

for $j = 1, \ldots, n$, where $u^*(s)$ is defined in (17), is the minimum-time control for the Problem 2 under Assumption 1.

*Proof:* Under Assumption 1, the result follows immediately by Bellman's Principle of Optimality. ■

## V. Compatible Selection of Cell Size for Given Vehicle Dynamics

The optimal control law of Proposition 2 is well defined only if the vehicle can reach any of the circular arcs $\mathcal{C}_j$ and $\mathcal{C}_{j+1}$ of the total composite path $\mathsf{P}(s)$ with the corresponding critical speed. For the sake of simplicity, in the sequel we shall investigate only curves that correspond to the boundary problem where the centers of the circles $\mathcal{C}_j$ and $\mathcal{C}_{j+1}$, are located at the midpoints of two different cell edges with a common vertex. This situation corresponds to the case when the length $\Sigma_{\mathcal{Y}_{j,j+1}} = \bar{s}_{j+1,2} - \bar{s}_{j,1}$ of the line segment $\mathcal{Y}_{j,j+1}$ is minimum. To this end, and without loss of generality, let us assume that $\rho_j \geq \rho_{j+1}$.

*Proposition 3:* The optimal feedback control of Proposition 2 is well defined only if the size $\ell$ of each cell and the radii of the circles $\mathcal{C}_j$ and $\mathcal{C}_{j+1}$, for $j = 1, \ldots, n$, satisfy the following conditions

$$\text{(i)} \quad \rho_{j+1} + \Delta\rho_j \leq \sqrt{2}/4\ell, \quad (20)$$

$$\text{(ii)} \quad \sqrt{\frac{1}{2}\ell^2 - (\Delta\rho_j)^2} \geq \frac{1}{2 f_t^{\max}}\big(2v_{\max}^2 - \quad (21)$$

$$f_r^{\max}(2\rho_{j+1} + \Delta\rho_j)\big), \quad \text{if } t_{\gamma_j} \in [\bar{t}_j, \bar{t}_{j+1}], \quad (22)$$

$$\text{(iii)} \quad \sqrt{\frac{1}{2}\ell^2 - (\Delta\rho_j)^2} \geq \frac{f_r^{\max}\Delta\rho_j}{2 f_t^{\max}} \quad (23)$$

$$\text{if } v(t) < v_{\max} \text{ for all } t \in [\bar{t}_j, \bar{t}_{j+1}],$$

where $\Delta\rho_j = \rho_j - \rho_{j+1}$.

*Proof:* Condition (20) is a well-posedness requirement for the path planning scheme introduced in Section III so that $\mathcal{C}_j$ and $\mathcal{C}_{j+1}$ do not overlap. Additionally, the boundary condition $v(s = \bar{s}_{j+1,2}) = v_{\mathsf{c}}^{\mathcal{C}_{j+1}}$, for $j = 1, \ldots, n$ is satisfied for the case when $t_{\gamma_j} \in [\bar{t}_{j,1}, \bar{t}_{j+1,2}]$ only if $s_{\delta_j} \in [s_{\gamma_j}, \bar{s}_{j+1,2}]$. It follows that

$$\Sigma_{\mathcal{Y}_{j,j+1}} \geq \frac{1}{2 f_t^{\max}}\left(2v_{\max}^2 - f_r^{\max}(2\rho_{j+1} + \Delta\rho_j)\right). \quad (24)$$

Similarly, for the case when $v(t) < v_{\max}$ for all $t \in [\bar{t}_j, \bar{t}_{j+1}]$ the boundary condition $v(s = \bar{s}_{j+1,2}) = v_{\mathsf{c}}^{\mathcal{C}_{j+1}}$ is satisfied only if

$$\Sigma_{\mathcal{Y}_{j,j+1}} \geq \frac{1}{2 f_t^{\max}}\left(\left(v_{\mathsf{c}}^{\mathcal{C}_j}\right)^2 - \left(v_{\mathsf{c}}^{\mathcal{C}_{j+1}}\right)^2\right) = \frac{f_r^{\max}\Delta\rho_j}{2 f_t^{\max}}. \quad (25)$$

With the aid of Fig. 5, we deduce that $\Sigma_{\mathcal{Y}_{j,j+1}} = \sqrt{\frac{1}{2}\ell^2 - (\Delta\rho_j)^2}$. The desired results follow immediately. ■

We observe that by increasing the difference $\Delta\rho_j$ between two successive circular arcs, the constraints (24) and (25) become more stringent, in the sense that the cell has to be sufficiently large.

## VI. Simulation Results

In order to demonstrate the efficiency of the proposed path planning scheme, we present simulation results for a non-trivial planning problem. We assume that the agent operates inside a supercell comprised of sixteen cells. In each figure the white cells correspond to free cells and the black ones to full cells. The grey cells are cells which are not inside the vehicle's sensors horizon at the particular time instant. The exact obstacle distribution inside the supercell is not known a priori. Instead, it becomes available as the agent proceeds to the desired configuration. As mentioned in the analysis of Section III-B, the exploration horizon is just three cells. In Figs. 6(a)-6(f) we see the path evolution (solid blue line) as the agent approaches the exit point with the appropriate orientation. Once a cell is visited by the agent, its color will remain white for a clearer demonstration of the path followed by the agent. For simplicity, the size of the circles used in

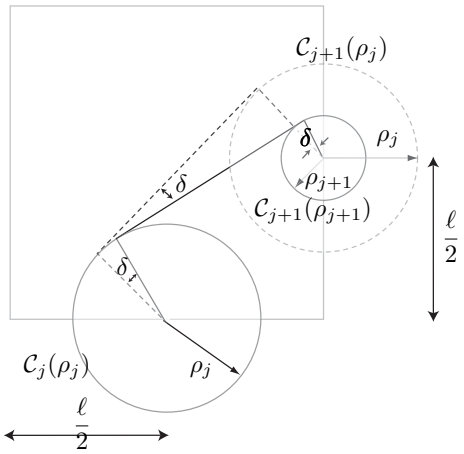


Fig. 5. By adjusting the radii of the circles $\mathcal{C}_j$ and $\mathcal{C}_{j+1}$ and by keeping the size of the cell fixed, it may be possible to satisfy the well-posedness requirement for the optimal policy of Proposition 2.

the simulation results is fixed for all maneuvers. Furthermore, in order to demonstrate a possible variation of the maneuver scheme depicted in Fig. 3 we have chosen to place the centers of the circles at one of the common vertices for any two adjacent, free cells.

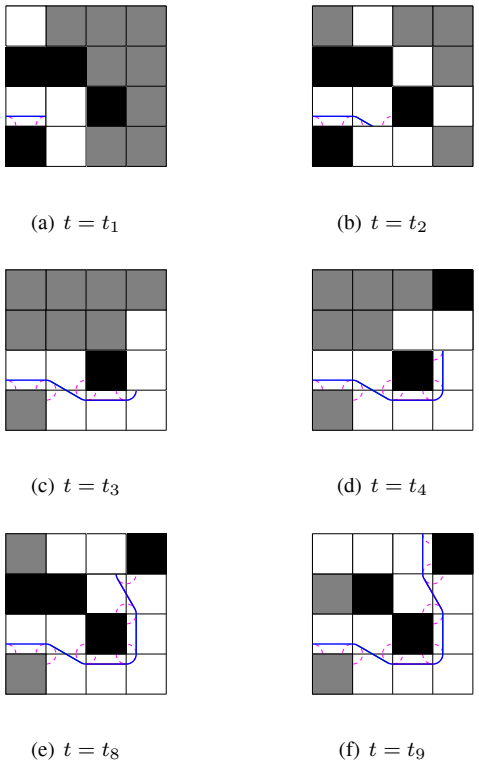

(a) $t = t_1$ (b) $t = t_2$

(c) $t = t_3$ (d) $t = t_4$

(e) $t = t_8$ (f) $t = t_9$

Fig. 6. Path evolution using the appropriate maneuvers.

## VII. Conclusions

In this paper we have presented an on-line trajectory generation scheme using path and motion primitives, which works with any rectangular cell-based path planning algorithm. We showed how the vehicle dynamics affect the geometric characteristics of the path and vice versa. We have proposed a geometric scheme that generates a composite path $\mathsf{P}(s)$ that is compatible to the given kinodynamic constraints. Subsequently, we solved analytically the minimum-time problem on this path, thus inducing a suitable time parameterization along the path $\mathsf{P}(s)$ that is compatible with the kinodynamic constraints. The resulting trajectory can be generated with minimal effort and can be tracked exactly by the vehicle.

**Acknowledgement:** This work has been supported in part by NSF (award no. CMS-0510259) and ARO (award no. W911NF-05-1-0331). The first author would like to thank Efstathios Velenis for his valuable comments concerning the minimum time trajectory generation.

## References

[1] L. E. Dubins, "On curves of minimal length with a constraint on average curvature, and with prescribed initial and terminal positions and tangents," *American Journal of Mathematics*, vol. 79, no. 3, 1957.

[2] H. J. Sussman, "Shortest 3-dimensional path with a prescribed curvature bound," in *Proceedings of 34th IEEE Conference on Decision and Control*, pp. 3306 – 3312, 1995.

[3] J. Reif and H. Wang, "The complexity of the two dimensional curvature-constrained shortest-path problem," in *Third International Workshop on Algorithmic Foundation of Robotics (WARF 98)*, (Houston, Texas), pp. 49–57, 1998.

[4] P. Jacobs and J. Canny, "Planning smooth paths for mobile robots," *Nonholonomic Motion Planning*, pp. 271–342, 1992.

[5] S. Bereg and D. Kirkpatrick, "Curvature-bounded traversals of narrow corridors," in *Proceedings of the twenty-first Annual Symposium on Computational Geometry*, (Pisa, Italy), pp. 278–287, 2005.

[6] J. Backer and D. Kirkpatrick, "Finding curvature-constrained paths that avoid polygonal obstacles," in *SCG '07*, (Gyeongju, South Korea), pp. 66–73, June 2007.

[7] K. G. Shin and N. D. McKay, "Minimum-time control of robotic manipulators with geometric path constraints," *IEEE Transactions on Automatic Control*, vol. 30, no. 6, pp. 531–541, 1985.

[8] J. E. Bobrow, S. Dubowsky, and J. S. Gibson, "Time-optimal control of robotic manipulators along specified paths," *International Journal of Robotics Research*, vol. 4, no. 3, pp. 3–17, 1985.

[9] J. Canny, A. Rege, and J. Reif, "An exact algorithm for kinodynamic planning in the plane," *Discrete and Computational Geometry*, pp. 461–482, 1991.

[10] E. Velenis and P. Tsiotras, "Minimum-time travel for a vehicle with acceleration limits: Theoretical analysis and receding horizon implementation," *Journal of Optimization Theory and Applications*, vol. 138, no. 2, pp. 275–296, 2008.

[11] E. Frazzoli, M. A. Dahleh, and E. Feron, "A hybrid control architecture for aggressive maneuvering of autonomous helicopters," in *Proceedings of 38th IEEE Conference on Decision and Control*, (Phoenix, Arizona), pp. 2471–2476, December 7-10 1999.

[12] E. Frazzoli, M. A. Dahleh, and E. Feron, "Maneuver-based motion planning for nonlinear systems with symmetries," *IEEE Transactions on Robotics*, vol. 21, pp. 1077–1091, December 2005.

[13] P. Tsiotras and E. Bakolas, "A hierarchical on-line path-planning scheme using wavelets," in *Proceedings of the European Control Conference*, (Kos, Greece), pp. 2806–2812, July 2–5 2007.

[14] E. Bakolas and P. Tsiotras, "Multiresolution path planning using sector decompositions compatible to on-board sensor data," in *Proceedings of the AIAA Guidance, Navigation and Control Conference and Exhibit*, (Honolulu, HI), Aug. 18–21 2008. AIAA Paper 2008-7238.